Photoprotection in a purple phototrophic bacterium mediated by oxygen-dependent alteration of carotenoid excited-state properties

Václav Šlouf[a], Pavel Chábera[b], John D. Olsen[c], Elizabeth C. Martin[c], Pu Qian[c], C. Neil Hunter[c], and Tomáš Polívka[a,d,1]

[a]Faculty of Science, University of South Bohemia, Branišovská 31, 370 05 České Budějovice, Czech Republic; [b]Department of Chemical Physics, Lund University, SE-222 41 Lund, Sweden; [c]Department of Molecular Biology and Biotechnology, University of Sheffield, Sheffield S10 2TN, United Kingdom; and [d]Biological Centre, Czech Academy of Sciences, Branišovská 31, 370 05 České Budějovice, Czech Republic

Edited by Robin M. Hochstrasser, University of Pennsylvania, Philadelphia, PA, and approved April 4, 2012 (received for review January 25, 2012)

Carotenoids are known to offer protection against the potentially damaging combination of light and oxygen encountered by purple phototrophic bacteria, but the efficiency of such protection depends on the type of carotenoid. *Rhodobacter sphaeroides* synthesizes spheroidene as the main carotenoid under anaerobic conditions whereas, in the presence of oxygen, the enzyme spheroidene monooxygenase catalyses the incorporation of a keto group forming spheroidenone. We performed ultrafast transient absorption spectroscopy on membranes containing reaction center-light-harvesting 1-PufX (RC-LH1-PufX) complexes and showed that when oxygen is present the incorporation of the keto group into spheroidene, forming spheroidenone, reconfigures the energy transfer pathway in the LH1, but not the LH2, antenna. The spheroidene/spheroidenone transition acts as a molecular switch that is suggested to twist spheroidenone into an s-*trans* configuration increasing its conjugation length and lowering the energy of the lowest triplet state so it can act as an effective quencher of singlet oxygen. The other consequence of converting carotenoids in RC-LH1-PufX complexes is that S_2/S_1/triplet pathways for spheroidene is replaced with a new pathway for spheroidenone involving an activated intramolecular charge-transfer (ICT) state. This strategy for RC-LH1-PufX-spheroidenone complexes maintains the light-harvesting cross-section of the antenna by opening an active, ultrafast S_1/ICT channel for energy transfer to LH1 Bchls while optimizing the triplet energy for singlet oxygen quenching. We propose that spheroidene/spheroidenone switching represents a simple and effective photoprotective mechanism of likely importance for phototrophic bacteria that encounter light and oxygen.

charge-transfer state | photoprotection | purple bacteria | photosynthesis

Carotenoids are natural pigments that absorb light in the 450–550 nm spectral region and transfer the energy to (bacterio) chlorophylls [(B)Chls] thereby acting as important energy donors in photosynthesis (1). In addition to extending the spectral range for absorption of solar energy, carotenoids play a structural role in light-harvesting (antenna) complexes (2, 3). Finally, carotenoids play a photoprotective role by dissipating unwanted excited states in antenna complexes (4, 5). It is well documented that carotenoids in purple phototrophic bacteria perform light-harvesting and structural roles, and the availability of carotenoidless mutants showed early on that carotenoids are essential for protection against oxygen radicals (6, 7). The present study demonstrates the mechanistic basis for photoprotection in photosynthetic bacteria using the purple bacterium *Rhodobacter (Rba.) sphaeroides* as a model. The photosynthetic complexes of this bacterium form interconnected membrane domains representing ~4,000 BChl molecules (8–10). The membranes are found within the cell as hundreds of spherical intracytoplasmic membrane vesicles ~50 nm in diameter (11). Light-harvesting LH2 complexes form the bulk light-harvesting antenna that donates energy to reaction center (RC)-LH1 complexes (12).

In terms of their light-harvesting function, it is now well-established that carotenoids have two excited states that serve as energy donors: the S_2 state, responsible for the strong absorption in the 400–550 nm region and the dark S_1 state, which is located below the absorbing state and is forbidden for one-photon transitions from the ground state (13). In LH2 complexes, the S_2 and S_1 states act as energy donors. The actual energy transfer efficiency, however, depends on the conjugation length N (the number of the conjugated C=C bonds) of the carotenoid. Whereas the S_2-mediated energy transfer is nearly constant (~50%) for carotenoids with $N = 9$–11 and decreases to ~30% only for $N > 12$ (1), the S_1 route reaches 90% efficiency for $N = 9$ and drops to less than 10% for $N > 11$ (14–16). This strong dependence is ascribed to unfavorable spectral overlap between the carotenoid S_1 state and Q_y band of BChl-*a* (1). Essentially the same situation was found for either native LH1 complexes (17) or LH1 reconstituted with different carotenoids (18) or for genetically modified LH2 complexes (19).

In other types of light-harvesting complexes such as the peridinin-chlorophyll protein from dinoflagellates, carotenoids with a conjugated C=O group facilitate S_1-mediated energy transfer by coupling to an intramolecular charge-transfer (ICT) state (20). This light-harvesting strategy seems common among certain genera of marine algae that utilize carbonyl carotenoids (21–23).

The existence of different paths of energy transfer from carotenoids in nature involving the S_1/S_2 or the S_1/ICT states raises the possibility that a biosynthetic transition from spheroidene to spheroidenone (see Fig. S1 for structures) in *Rba. sphaeroides*, known to occur when anaerobically grown cells are aerated, could act as a molecular "switch" to a photoprotective mode. Spheroidenone is known to be very effective in protecting against singlet oxygen (24). Furthermore, photostability studies on spheroidenone-containing LH1 and LH2 complexes in the presence of oxygen, and attached to gold surfaces in the membrane-bound or purified state, showed a remarkable resilience but only for the LH1 complex (25, 26). In the present study, we used an LH2-minus *crtA* mutant that only contains spheroidene to demonstrate that in anaerobic, photosynthetic cells energy transfer in membrane-bound RC-LH1-PufX complexes proceeds via the S_1/S_2 states. When oxygen is present, the CrtA enzyme spheroidene monooxygenase present in the wild-type bacterium catalyses the incorporation of a keto group forming spheroidenone (27), which transforms energy transfer within the LH1 complex by

Author contributions: C.N.H. and T.P. designed research; V.S., P.C., E.C.M., and P.Q. performed research; V.S. and T.P. analyzed data; and V.S., J.D.O., C.N.H., and T.P. wrote the paper.

The authors declare no conflict of interest.

This article is a PNAS Direct Submission.

[1]To whom correspondence should be addressed. E-mail: polivka@ufb.jcu.cz.

This article contains supporting information online at www.pnas.org/lookup/suppl/doi:10.1073/pnas.1201413109/-/DCSupplemental.

shutting off ultrafast triplet formation and initiating an S_1/ICT pathway. Furthermore, a specific spheroidenone configuration in LH1 decreases the energy of the triplet state, promoting photoprotective quenching of triplet BChl, or singlet oxygen. This effect is specific for the RC-LH1-PufX complex and is not observed for the peripheral LH2 complex. We propose that spheroidene/spheroidenone switching in RC-LH1-PufX complexes represents a simple and effective photoprotective mechanism of likely importance for phototrophic bacteria that encounter light and oxygen.

Results and Discussion

Absorption spectra of membrane-bound RC-LH1-PufX complexes containing spheroidene or spheroidenone, hereafter referred to as RC-LH1-PufX(sph) and RC-LH1-PufX(spn), respectively, are shown in Fig. 1. The PufX polypeptide is an integral component of the *Rba. sphaeroides* RC-LH1 core complex and is essential for efficient photosynthetic growth (28). The spectra are dominated by BChl-*a* Q_y and Soret bands peaking at ~876 and ~372 nm, respectively; the BChl-*a* Q_x band appears at 590 nm. The RC contributions to the absorption spectra are also very similar in both complexes. The BChl monomers in the RC give rise to ~805-nm bands whereas those around ~760 nm are due to RC bacteriopheophytins (29). Differences between the RC-LH1-PufX complexes are most pronounced in the blue-green region where carotenoids absorb. Spheroidene has three well-resolved vibrational bands in the RC-LH1-PufX(sph) complex. The lowest energy transition due to the 0-0 band is readily identified at 507 nm. The absorption spectrum of spheroidenone in the RC-LH1-PufX(spn) complex is shifted to longer wavelengths; moreover, the resolution of its vibrational bands is significantly diminished as seen in other LH complexes binding the carbonyl carotenoid spheroidenone (14, 15) or okenone (30). The weakly pronounced 0-0 band of spheroidenone in RC-LH1-PufX(spn) appears at ~545 nm.

Intramolecular Charge-Transfer State in RC-LH1-PufX Complexes. To search for possible identifiers of an ICT state in RC-LH1-PufX complexes, we recorded transient absorption spectra after excitation of carotenoids at 475 nm (spheroidene) and 514 nm (spheroidenone). Fig. 2*A* shows a comparison of transient absorption spectra of both complexes recorded at 500 fs after excitation. The spectrum of the RC-LH1-PufX(sph) complex is dominated by a band at 553 nm that is typical of the S_1–S_n band of spheroidene (14, 15). In addition, a shoulder appears on the high-energy side of the main peak that we attribute to the transition associated with the S^* state (31); however, the transient absorption spectrum of the RC-LH1-PufX(spn) complex is significantly different, and a new spectral band reminiscent of the ICT-like transition of carbonyl carotenoids in polar solvents (32, 33) is observed around 750 nm. Although the broadening of the S_1–S_n transition of spheroidenone is observed in LH2 complexes, the band at 750 nm has never been observed in LH2 (14, 15), though a similar, but much weaker, band was detected in the spheroidenone-containing LH4 antenna of *Roseobacter denitrificans* (34).

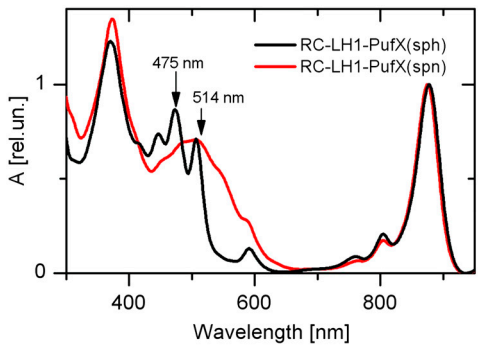

Fig. 1. Absorption spectra of RC-LH1-PufX complexes containing spheroidene (sph) and spheroidenone (spn). The excitation wavelengths are indicated by vertical arrows.

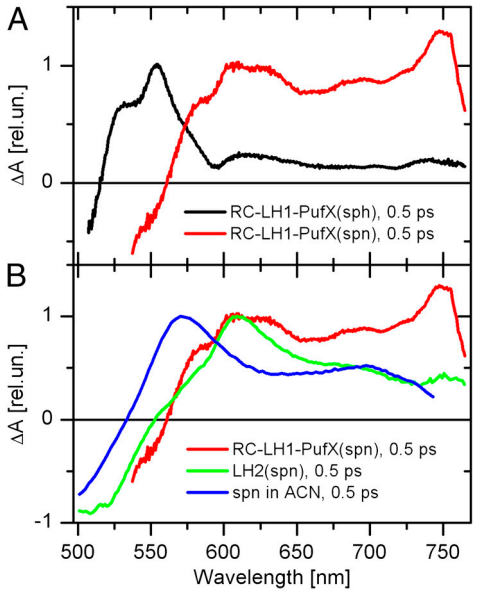

Fig. 2. Transient absorption spectra recorded after excitation of the S_2 state of carotenoid in (*A*) RC-LH1-PufX complexes containing spheroidene (sph) and spheroidenone (spn). The transient absorption spectra were recorded 0.5 ps after excitation at 475 nm (sph) and 514 nm (spn). (*B*) Comparison of transient absorption spectra of the RC-LH1-PufX(spn) complex, LH2 complex containing spn, and spn in acetonitrile. Excitation wavelengths were 514 nm (RC-LH1-PufX), 515 nm (LH2), and 500 nm (acetonitrile). Data on LH2 and spheroidenone in solution are taken from refs. 15 and 33. All spectra are normalized to S_1–S_n maximum.

In Fig. 2*B*, we compare the transient absorption spectra of spheroidenone in acetonitrile and in the RC-LH1-PufX(spn) and LH2 complexes. It is clear that spheroidenone in LH2 resembles that in solution exhibiting only a weak feature around 690 nm attributable to the ICT-S_n transition. On the other hand, in RC-LH1-PufX(spn) the ICT-S_n transition of spheroidenone is far more intense and shifted to ~750 nm. Thus, binding of spheroidenone to the RC-LH1-PufX complex stabilizes the ICT state that consequently must play a role in excited-state dynamics. Because no such effect is observed in spheroidenone-containing LH2 complexes, there must be significant differences in spheroidenone-protein interactions between RC-LH1-PufX and LH2 complexes of *Rba. sphaeroides*. Because a high-resolution atomic structure of the RC-LH1-PufX complex is not available, it is not possible to identify the origin of the difference between RC-LH1-PufX and LH2 complexes from structural data. Yet, there are spectroscopic indicators that allow us to hypothesize about possible origins of the observed differences in excited-state properties.

First, it must be noted that the intensity of the ICT-like transition of spheroidenone in the RC-LH1-PufX(spn) complex is significantly stronger than that observed in the most polar solvents (Fig. 2*B*). Although it is possible to separate the S_1-like and ICT-like transitions in transient absorption spectra, the S_1 and ICT states of carbonyl carotenoids are strongly coupled in the S_1/ICT state (32, 35), and the intensity of the ICT-like transition is a measure of a degree of charge-transfer character of the S_1/ICT state. It was recently shown that the intensity of the ICT-like transition significantly increases if a single conjugated carbonyl group of a carotenoid is positioned in an s-*trans* configuration with respect to the main conjugated backbone (36); however, this is not the case for spheroidenone in solution where the carbonyl group is in an s-*cis* orientation as evidenced by molecular

modeling showing that s-*cis* configuration is far more stable (Fig. S2). Consequently, the significantly stronger ICT band in the RC-LH1-PufX(spn) complex could be explained if the binding site in the RC-LH1-PufX(spn) "twists" the carbonyl group of spheroidenone into the s-*trans* configuration (Fig. S2).

Further support for this hypothesis is provided by a comparison of transient absorption spectra of spheroidenone in the RC-LH1-PufX(spn) complex with those of the carotenoid hydroxyechinenone in the orange carotenoid protein (OCP) from cyanobacteria that exhibits very similar behavior. Whereas no ICT-like transitions are detected for hydroxyechinenone in solution, a red-shifted ICT band dominates the transient absorption spectrum of hydroxyechinenone bound to OCP (37). Unlike the RC-LH1-PufX complex, the atomic structure of OCP has been determined to 1.65 Å resolution (38), allowing identification of the changes leading to "activation" of the ICT state. The carbonyl group of hydroxyechinenone is in the s-*cis* orientation in solution minimizing the charge-transfer character of the S_1/ICT state (36); however, the hydroxyechinenone binding site in OCP forces the terminal 4-keto-β-ionylidene ring of hydroxyechinenone to twist, aligning the conjugated carbonyl group into the s-*trans* orientation with respect to the rest of the conjugated bond system (37). Moreover, the conjugated carbonyl group of hydroxyechinenone in OCP forms hydrogen bonds to nearby tryptophan and tyrosine residues. These structural changes result in the appearance of the ICT band in the transient absorption spectrum; however, it disappears in the closely related red carotenoid protein, where the part of the protein forming the carbonyl binding site in OCP is missing (39).

Thus, comparison of data recorded for the RC-LH1-PufX(spn) complex and the OCP protein suggests that a conformational change of spheroidenone in RC-LH1-PufX(spn), which does not occur in LH2, causes the enhancement of the charge-transfer character of the S_1/ICT state of spheroidenone resulting in observation of the ICT-like band at 750 nm. It is likely that hydrogen bonding to the carbonyl group also contributes to this effect, however, hydrogen bonding alone cannot generate an ICT band of such magnitude, as is seen when comparing the intensity of the ICT band of spheroidenone in the hydrogen-bonding solvent methanol (32) and in aprotic acetonitrile (33). The ICT bands in both solvents are weak and of comparable magnitude. Thus, the magnitude of the ICT band of spheroidenone in RC-LH1-PufX (spn) complexes cannot be reproduced in any solvent suggesting that the introduction of the keto group probably twists the carotenoid molecule, a significant structural change that has to be accommodated by an alteration of the binding site within the LH1 complex.

Based on the arguments presented above, we propose that spheroidenone bound to the RC-LH1-PufX(spn) complex of *Rba. sphaeroides* has the keto group in the s-*trans* orientation, whereas the s-*cis* orientation most likely occurs in LH2. In addition, hydrogen bonding of LH1 side chains to the carbonyl oxygen may further enhance the charge-transfer character of the S_1/ICT state of spheroidenone in the RC-LH1-PufX(spn) complex.

Carotenoid Excited-State Dynamics. Having established that the 750 nm band in transient absorption spectra of the RC-LH1-PufX(spn) complex arises from the ICT state, we may proceed with an analysis of excited-state dynamics. Results of global fitting data recorded for both RC-LH1-PufX complexes are shown in Fig. 3. For the RC-LH1-PufX(spn) complex (Fig. 3*A*), the first evolution associated difference spectrum (EADS) corresponding to the S_2 state decays in <0.1 ps to the second EADS (red), which is clearly due to the S_1/ICT state, because it contains S_1-like (600 nm) and ICT-like (750 nm) transitions. Interestingly, this second EADS contains only a weak signal attributable to Q_x bleaching (~590 nm) suggesting that the S_2 channel is of minor importance in this complex. This also implies that $S_2 - S_1$/ICT

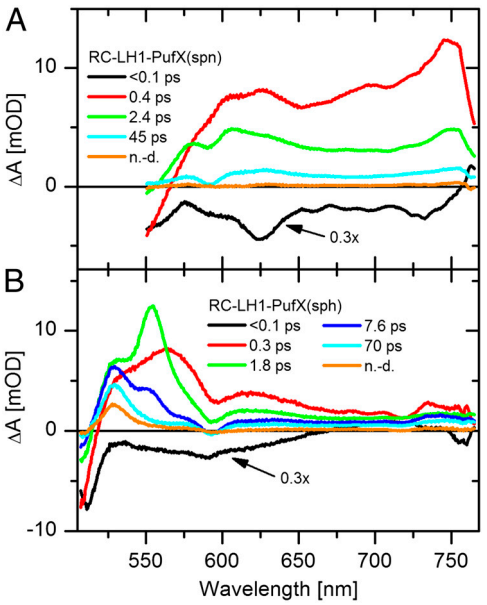

Fig. 3. EADS resulting from global fitting the data in the visible spectral region measured for (*A*) RC-LH1-PufX(spn) and (*B*) RC-LH1-PufX(sph) complexes. The data at wavelengths shorter than 550 nm are omitted for the RC-LH1-PufX(spn) complex due to strong scattering from excitation. n.d., nondecaying component.

internal conversion occurs in s-*trans* spheroidenone in the RC-LH1-PufX(spn) complex significantly faster than for spheroidene in the RC-LH1-PufX(sph) complex. This observation agrees with a previous study of S_2 decay of hydroxyechinone where activation of the ICT state significantly shortens the S_2 lifetime in the OCP in comparison with the lifetime in solution (37). The S_1/ICT state decays in 0.4 ps during which process the appearance of a dip is clearly visible, superimposed on the broad S_1–S_n transition. This feature is due to the Q_x bleaching and identifies the 0.4 ps process as energy transfer from the S_1/ICT state. The next EADS decays in 2.4 ps. The EADS generated by the 2.4 ps process (cyan) does not contain any spheroidenone bleaching and is, thus, solely due to BChl-*a*. The 45 ps time constant of the decay of this EADS is associated with the overall trapping time of excited states in these photosynthetic membranes. It is important to note that the monomer/dimer status of the spheroidenone complexes has no influence on the carotenoid excited-state dynamics. The activation of the ICT state and excited-state dynamics of spheroidenone in the PufX-minus and PufX-containing RC-LH1 (spn) complexes are essentially identical (Fig. S3).

Global analysis of data measured for the RC-LH1-PufX(sph) complex (Fig. 3*B*) reveals that the S_2 state decays on the sub-100 fs timescale (black EADS). When going to the next EADS (red), the clear dip around 590 nm indicates that the S_2-mediated energy transfer is far more important here, in comparison with the RC-LH1-PufX(spn) complex. This EADS decays in 0.3 ps, which is nearly the same time constant as for RC-LH1-PufX (spn); but, the spectral properties are qualitatively different as it exhibits the characteristics of a hot S_1 state (15, 40). The pathway from the hot S_1 state of carotenoids has been observed in other LH complexes (31, 41, 42). Whether or not this energy transfer channel is active in RC-LH1-PufX(sph) needs to be elucidated by complementary measurements of BChl-*a* dynamics in the near-IR spectral region. The EADS of the hot S_1 state relaxes to form the EADS associated with the S_1 state (green) which decays in 1.8 ps. The shape of the next EADS (blue) is reminiscent of the S^* state (31). The last dynamic process (cyan to orange EADS) occurs with a 70 ps time constant and, again, reflects the overall trapping time for these membranes. At present, we cannot explain the slower trapping time for RC-LH1-PufX(sph) than for

RC-LH1-PufX(spn) membranes, and a systematic study of trapping times in the presence of LH2 complexes will be required to examine this point further. The final, nondecaying EADS of the RC-LH1-PufX(sph) contains a clear band at 530 nm that arises from the triplet state of spheroidene.

Carotenoid to BChl-a Energy Transfer. In order to confirm that the 0.4 ps (spheroidenone) and 0.3 and 1.8 ps (spheroidene) components observed in the visible spectral region are associated with energy transfer, we carried out experiments probing the near-IR region, monitoring the signal of the BChl-*a* Q_y band. The global fitting results are depicted in Fig. 4. For membranes containing the RC-LH1-PufX(spn) complex (Fig. 4*A*), the first EADS (red) contains some BChl-*a* signal but its contribution is smaller in comparison with the RC-LH1-PufX(sph) sample (Fig. 4*B*). This observation confirms the hypothesis that the S_2 state of spheroidenone is a minor donor of excitation energy for BChl-*a* in RC-LH1-PufX(spn) complexes. The magnitude of the BChl-*a* bleaching in the near-IR region increases greatly with a 0.6 ps component that matches the 0.4 ps component associated with the S_1/ICT state observed in the visible region. Thus, energy transfer from spheroidenone to BChl-*a* in the RC-LH1-PufX(spn) complex proceeds predominantly via the S_1/ICT route. The second EADS (green) decays with a 2.5 ps component. During this process, there is only a slight decrease of the BChl-*a* signal indicating that no energy transfer occurs with this time constant. Virtually the same component of 2.4 ps was observed in the visible region (Fig. 3*A*), and its presence in the near-IR region indicates that it is associated with BChl-*a* dynamics. Indeed, the 2.4 ps EADS in the visible region has a shape similar to the 45 ps EADS except in its intensity and is clearly due to BChl-*a* (Fig. 3*A*). The next EADS (cyan) has a lifetime of 44 ps and evidently corresponds to the trapping time in RC-LH1-PufX(spn) complex.

Fig. 4*B* shows the EADS obtained from global fits of the data measured in the near-IR region for the RC-LH1-PufX(sph) complex. Unlike the RC-LH1-PufX(spn) complex, the first EADS (black) already contains a significant BChl-*a* bleaching component that increases further during the <100 fs step. These observations indicate that a substantial part of the energy is transferred from the S_2 state of spheroidene. A further increase (red to green EADS) is characterized by a 0.3 ps component that matches the decay of the hot S_1 state observed in the visible region (Fig. 3*B*) supporting the notion of energy transfer via the hot S_1 state of spheroidene. The green EADS has a 1.7 ps lifetime, and the process associated with this component increases the BChl-*a* signal further. The match between this time constant and that observed in the visible region allows an assignment as energy transfer from the relaxed S_1 state of spheroidene. During the next process associated with the 7 ps time constant, the cyan EADS is formed. Because it is accompanied by the decrease of the BChl-*a* signal, this EADS is most probably associated with relaxation of BChl-*a* excited states. Although it would be tempting to couple the ~7 ps time constants in the visible and near-IR regions, the dominating processes are most probably unrelated. Whereas the near-IR decrease of the signal is unequivocally associated with BChl-*a* relaxation, the 7.6 ps EADS in the visible region exhibits characteristic carotenoid features. The cyan EADS decays with an 80 ps time constant, again, due to trapping events in RC-LH1-PufX (sph) complex.

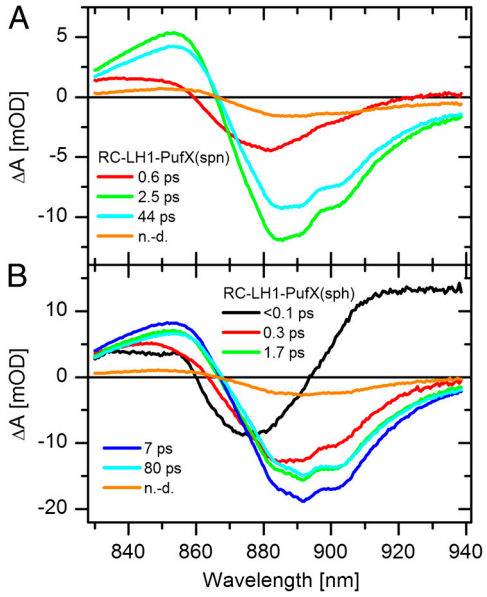

Fig. 4. EADS resulting from global fitting the data in the near-IR spectral region measured for (*A*) RC-LH1-PufX(spn), (*B*) RC-LH1-PufX(sph) complexes. n.d., nondecaying component.

Thus, three energy transfer pathways, via the S_2, hot S_1 and relaxed S_1 states, are active in the RC-LH1-PufX(sph) complex whereas only two pathways mediated by the S_1/ICT state, and to a lesser extent by S_2, exist in RC-LH1-PufX(spn) complex (see Fig. S4 for a scheme of energy transfer pathways). Multiple pathways involving S_2 and S_1 routes are common in LH2 and LH1 complexes of purple bacteria binding carotenoids with $N < 11$ (1, 15, 18). When carotenoids with a longer conjugated bond system such as lycopene (16, 18, 19) or spirilloxanthin (18, 31) are bound to LH2 or LH1 complexes the S_1 route becomes inactive, but the S_2 pathway is functional in all purple bacterial antenna studied so far. It is worth noting that the S_2 route is significantly diminished in light-harvesting complexes of dinoflagellates or diatoms binding the carbonyl carotenoids peridinin or fucoxanthin. Then, the pathway through the S_1/ICT state becomes the major pathway (20–22) reminiscent of the situation studied here in RC-LH1-PufX(spn) complexes.

The RC-LH1-PufX(spn) complex represents a unique light-harvesting system among purple bacteria. The biosynthetic incorporation of a single keto oxygen into the structure of spheroidene changes the energy transfer pathways, and the S_1/ICT route becomes dominant. Because the ICT state is not active in LH2 complexes binding the same carotenoid, spheroidenone, an LH1-specific interaction must exist between the keto group of spheroidenone and amino acid residues such as tryptophan and tyrosine, as found for interactions of these residues with LH1 BChls (43, 44). There is evidence that the Trp residue of the highly conserved Lys-Ile-Trp (KIW) motif found in the N-terminal domain of the LH1α polypeptide plays a role in binding spheroidenone in the LH1 complex of *Rba. capsulatus* (45, 46); however, the same KIW motif is found in LH2, and no ICT state is found in this complex. It is possible that the neighboring αTyr-27 residue provides the hydrogen bond to the C2 keto group of spheroidenone that stabilizes the s-*trans* configuration as the corresponding residue in LH2 is a Gly.

Carotenoid Triplet State Formation in RC-LH1-PufX Complexes. The transient absorption data in Fig. 2*A* and the EADS in Fig. 3 show that the blue parts of these spectra differ significantly in the two RC-LH1-PufX complexes. Whereas spheroidenone bleaching dominates below 560 nm, the transient absorption spectrum of the RC-LH1-PufX(sph) complex contains a positive signal below 540 nm that does not decay within the time window of the experiment. This nondecaying signal forms a narrow peak centered at 530 nm and is generated within the first picosecond after excitation. The same signal was observed in LH1 complexes of *Rhodospirillum rubrum* reconstituted with spheroidene, and it was identified as a T_1–T_n transition due to a spheroidene triplet state (18).

However, the observed picosecond dynamics of the 530 nm band are not consistent with known lifetimes of the triplet state.

Thus, Papagiannakis *et al.* (31) interpreted the early signal as arising from the S^* state that is the precursor of the triplet state in native LH complexes of *Rba. sphaeroides*. In fact, the time constants extracted here from global fitting of the RC-LH1-PufX (sph) data are remarkably similar to those obtained for LH2 complex from the same organism (31). Consequently, we assign the 7.6 ps component to decay of the S^* state, formed from the S_2 state of spheroidene. Because the process associated with the 7.6 ps component is accompanied by a loss of ground state bleaching (Fig. 3*B*), it implies that the S^* state decays into triplet and ground states. Comparing the amplitudes of the components obtained here (Fig. 3*B*) and in LH2 (31), the branching ratio is shifted more towards the triplet state in RC-LH1-PufX(sph) complex. The underlying dynamics are, however, essentially identical in RC-LH1-PufX(sph) and LH2(sph) complexes.

Whereas in the RC-LH1-PufX(sph) complex the resulting triplet yield is higher than in corresponding LH2 complexes, the change of spheroidene to spheroidenone that involves only the addition of a keto group to the carotenoid conjugated system switches off the pathway toward the triplet state completely. Although the scattering prevents the inclusion of <550 nm data in the global fitting (Fig. 3*A*), comparison of transient absorption spectra at 100 ps recorded for RC-LH1-PufX(sph) and RC-LH1-PufX(spn) complexes (Fig. S5) clearly shows that no triplet signal is observed in the RC-LH1-PufX(spn) complex. Consequently, incorporation of spheroidenone in RC-LH1-PufX(spn) not only alters energy transfer pathways but also prevents ultrafast triplet formation.

A Possible Biological Role For Spheroidene/Spheroidenone Conversion in Photosynthetic Bacteria. The conversion of spheroidene to spheroidenone mediated by spheroidene monooxygenase alters the conformation of the carotenoid, which twists in the s-*trans* configuration that is likely stabilized by a hydrogen-bonding interaction within the LH1 binding site. The effect of this change is to increase the conjugation length of the carotenoid, lowering the energy of the lowest triplet state (47) so it can act as an effective quencher of singlet oxygen and/or BChl-*a* triplet states. The other consequence of the conversion of spheroidene to spheroidenone is a modification of the energy transfer properties of RC-LH1-PufX complexes, which switch from an S_2/S_1/triplet mechanism to one involving mainly the S_1/ICT state. The s-*trans* configuration of spheroidenone leads to activation of the ICT state that maintains an active S_1-channel for energy transfer to LH1 Bchls while allowing the triplet energy drop to effectively quench singlet oxygen. This functional flexibility contrasts with that of lycopene, which has effective conjugation comparable to spheroidenone in s-*trans* configuration, and is found in some other light-harvesting complexes (48). This carotenoid evidently has an ideal triplet energy for scavenging singlet oxygen and, indeed, lycopene is the most effective carotenoid for singlet oxygen scavenging (49); however, the S_1 energy of lycopene is too low to transfer energy to BChl-*a* (1, 16).

The basis for the biological role of this process probably originates in the differing levels of light and oxygen encountered by purple phototrophic bacteria. As they move from a low-light, anaerobic environment to one nearer the surface where the light and oxygen levels increase, there is a need to protect the photosynthetic apparatus. Similar requirements are found in the aerobic anoxygenic phototrophs that represent almost 10% of microbes in the oceans (50). The proposed quenching mechanism offers effective protection against singlet oxygen without sacrificing the light-harvesting cross-section of the antenna, in line with work on other systems involving the ICT state (20). Quenching of BChl-*a* triplet states that may lead to singlet oxygen formation or quenching the singlet oxygen itself are of vital importance in conditions when light and oxygen is present. This is underlined by the recent study of Magis et al. (26) that compared the photostability of surface-immobilized LH1 and LH2 complexes with spheroidenone as the major carotenoid. LH1 complexes withstood 180 min of irradiation at 650 $W{\cdot}cm^{-2}$, whereas LH2 complexes were destroyed in less than 2 min. Thus, the ability of spheroidenone to optimize triplet energy in RC-LH1-PufX(spn) complexes and simultaneously maintain energy transfer channel between spheroidenone and BChl-*a* is a vital environmental response mechanism for this bacterium and likely for the many other phototrophic bacteria that also contain spheroidenone. In conclusion, we suggest that spheroidene/spheroidenone conversion in RC-LH1-PufX complexes represents a simple and effective photoprotective mechanism, to add to other photoprotective mechanisms found in nature such as the OCP of cyanobacteria and the xanthophyll cycle of plants.

Materials and Methods

Preparation of Intracytoplasmic Membranes. The *Rba. sphaeroides* deletion strain DD13 was complemented with the plasmid p(RKEHWT) (51). The resultant transconjugant DD13[pRKEHWT] contains WT RC-LH1-PufX core complexes but no LH2 complexes. Cultures of this strain were grown in the dark semiaerobically at 30 °C with shaking so that the carotenoid spheroidenone was incorporated into the core complexes. The LH2-minus *crtA* mutant DBCΩ Δ*crtA* was constructed by in-frame deletion of the *crtA* gene using an LH2-minus background, DBCΩ (51), so spheroidene became the dominant carotenoid in the core complexes; this mutant was grown photosynthetically. Intracytoplasmic membrane vesicles were then prepared from both LH2-minus mutants according to published methods (43). PufX-minus (see *SI Text*) membranes were prepared from a PufX-minus mutant with monomeric core complexes (52).

Time-resolved spectroscopy. The femtosecond laser setup is based on mode-locked Ti:sapphire oscillator (Tsunami, Spectra Physics) and Nd:YLF pumped Ti:sapphire amplifier (Spitfire Pro XP, Spectra Physics) with central output wavelength of 795 nm and 1 kHz repetition rate (6 mJ per pulse) delivering ~80 fs pulses. The output beam was split into two parts: one for pumping a collinear optical parametric amplifier (TOPAS-C, Light Conversion) to generate the pump beam, and the second one was led through a computer-controlled delay line and focused onto a 2-mm sapphire plate to generate a white light continuum. Subsequently, the probe pulses were split into two parts: the former overlapping with the pump pulse in the sample volume and the latter serving as a reference while not passing through the sample. The probe and the reference beams were then brought to the slit of a spectrograph and dispersed onto a double photodiode array, each with 512 elements. All samples were measured in a quartz shaking cuvette preventing sample degradation caused by long-term exposure to laser light. The intensity of excitation pulses was kept below 4.10^{14} $photons{\cdot}pulse^{-1}{\cdot}cm^{-2}$. Absorption spectra were measured before and after experiments to check for possible sample degradation, which did not exceed 6% in any case. Mutual polarization between pump and probe beams was set to the magic angle (54.7°). All data from time-resolved measurements were fitted globally (DA-Fit, Pascher Instruments) to a sum of exponentials using a sequential kinetic scheme with increasing lifetimes (53).

ACKNOWLEDGMENTS. The authors thank Harry Frank for providing data on LH2 complex shown in Fig. 2*B*. Research in the Czech Republic was supported by grants from the Czech Ministry of Education (MSM6007665808 and AV0Z50510513) and the Czech Science Foundation (P205/11/1164). V.Š. thanks the Grant Agency of the University of South Bohemia (027/2011/P) for financial support. C.N.H., E.C.M., P.Q., and J.D.O. gratefully acknowledge funding from the Biotechnology and Biological Sciences Research Council (UK). C.N.H. was also supported as part of the Photosynthetic Antenna Research Center (PARC), an Energy Frontier Research Center funded by the US Department of Energy, Office of Science, and Office of Basic Energy Sciences under Award Number DE-SC0001035.

1. Polívka T, Frank HA (2010) Molecular factors controlling photosynthetic light harvesting by carotenoids. *Acc Chem Res* 43:1125–1134.
2. Lang HP, Hunter CN (1994) The relationship between carotenoid biosynthesis and the assembly of the light-harvesting LH2 complex in *Rhodobacter sphaeroides*. *Biochem J* 298:197–205.
3. Plumley FG, Schmidt GW (1987) Reconstitution of chlorophyll a/b light-harvesting complexes—xanthophyll-dependent assembly and energy transfer. *Proc Natl Acad Sci USA* 84:146–150.
4. Demmig-Adams B, Adams WW (1996) The role of xanthophyll cycle carotenoids in the protection of photosynthesis. *Trends Plant Sci* 1:21–26.

5. Wilson A, et al. (2008) A photoactive carotenoid protein acting as light intensity sensor. *Proc Natl Acad Sci USA* 105:12075–12080.
6. Sistrom WR, Griffiths M, Stanier RY (1956) The biology of a photosynthetic bacterium which lacks coloured carotenoids. *J Cell Comp Physiol* 48:473–516.
7. Clayton RK, Smith C (1960) *Rhodopseudomonas sphaeroides*: high catalase and blue-green double mutants. *Biochem Biophys Res Commun* 3:143–145.
8. Hunter CN, Kramer HJM, van Grondelle R (1985) Linear dichroism and fluorescence emission of antenna complexes during photosynthetic unit assembly in *Rhodopseudomonas sphaeroides*. *Biochim Biophys Acta* 807:44–51.
9. Frese RN, et al. (2004) The long-range organization of a native photosynthetic membrane. *Proc Natl Acad Sci USA* 101:17994–17999.
10. Şener MK, Olsen JD, Hunter CN, Schulten K (2007) Atomic-level structural and functional model of a bacterial photosynthetic membrane vesicle. *Proc Natl Acad Sci USA* 104:15723–15728.
11. Tucker JD, et al. (2010) Membrane invagination in *Rhodobacter sphaeroides* is initiated at curved regions of the cytoplasmic membrane, then forms both budded and fully detached spherical vesicles. *Mol Microbiol* 76:833–847.
12. Sundström V, Pullerits T, van Grondelle R (1999) Photosynthetic light-harvesting: Reconciling dynamics and structure of purple bacterial LH2 reveals function of photosynthetic unit. *J Phys Chem B* 103:2327–2346.
13. Polívka T, Sundström V (2004) Ultrafast dynamics of carotenoid excited states: From solution to natural and artificial systems. *Chem Rev* 104:2021–2071.
14. Polívka T, Pullerits T, Frank HA, Cogdell RJ, Sundström V (2004) Ultrafast formation of a carotenoid radical in LH2 antenna complexes of purple bacteria. *J Phys Chem B* 108:15398–15407.
15. Cong H, et al. (2008) Ultrafast time-resolved carotenoid to bacteriochlorophyll energy transfer in LH2 complexes from photosynthetic bacteria. *J Phys Chem B* 112:10689–10703.
16. Zhang JP, et al. (2000) Mechanism of the carotenoid-to-bacteriochlorophyll energy transfer via the S_1 state in the LH2 complexes from purple bacteria. *J Phys Chem B* 104:3683–3691.
17. Rademaker H, Hoff AJ, van Grondelle R, Duysens LNM (1980) Carotenoid triplet yields in normal and deuterated *Rhodospirillum rubrum*. *Biochim Biophys Acta* 592:240–257.
18. Akahane J, Rondonuwu FS, Fiedor L, Watanabe Y, Koyama Y (2004) Dependence of singlet-energy transfer on the conjugation length of carotenoids reconstituted into the LH1 complex from *Rhodospirillum rubrum* G9. *Chem Phys Lett* 393:184–191.
19. Billsten HH, et al. (2002) Dynamics of energy transfer from lycopene to bacteriochlorophyll in genetically-modified LH2 complexes of *Rhodobacter sphaeroides*. *Biochemistry* 41:4127–4136.
20. Zigmantas D, Hiller RG, Sundström V, Polívka T (2002) Carotenoid to chlorophyll energy transfer in the peridinin-chlorophyll-*a*-protein complex involves an intramolecular charge transfer state. *Proc Natl Acad Sci USA* 99:16760–16765.
21. Polívka T, Hiller RG, Frank HA (2007) Spectroscopy of the peridinin-chlorophyll-a protein: Insight into light-harvesting strategy of marine algae. *Arch Biochem Biophys* 458:111–120.
22. Papagiannakis E, van Stokkum IHM, Fey H, Buchel C, van Grondelle R (2005) Spectroscopic characterization of the excitation energy transfer in the fucoxanthin-chlorophyll protein of diatoms. *Photosynth Res* 86:241–250.
23. Polívka T, et al. (2006) Energy transfer in the major intrinsic light-harvesting complex from *Amphidinium carterae*. *Biochemistry* 45:8516–8526.
24. Glaeser J, Klug G (2005) Photo-oxidative stress in *Rhodobacter sphaeroides*: Protective role of carotenoids and expression of selected genes. *Microbiology* 151:1927–1938.
25. Magis JG, et al. (2010) Light harvesting, energy transfer and electron cycling of a native photosynthetic membrane adsorbed onto a gold-surface. *Biochim Biophys Acta Biomembr* 1798:637–645.
26. Magis JG, et al. (2011) Use of engineered unique cysteine residues to facilitate oriented coupling of proteins directly to a gold substrate. *Photochem Photobiol* 87:1050–1057.
27. Yeliseev AA, Eraso JM, Kaplan S (1996) Differential carotenoid composition of the B875 and B800-850 photosynthetic antenna complexes in *Rhodobacter sphaeroides* 2.4.1: Involvement of spheroidene and spheroidenone in adaptation to changes in light intensity and oxygen availability. *J Bacteriol* 178:5877–5883.
28. Farchaus JW, Barz WP, Grunberg H, Oesterhelt D (1992) Studies on the expression of the pufX polypeptide and its requirement for photoheterotrophic growth in *Rhodobacter sphaeroides*. *EMBO J* 11:2779–2788.
29. Pan J, et al. (2011) Carotenoid excited-state properties in photosynthetic purple bacterial reaction centers: Effects of the protein environment. *J Phys Chem B* 115:7058–7068.
30. Andersson PO, Cogdell RJ, Gillbro T (1996) Femtosecond dynamics of carotenoid-to-bacteriochlorophyll a energy transfer in the light-harvesting antenna complexes from the purple bacterium *Chromatium purpuratum*. *Chem Phys* 210:195–217.
31. Papagiannakis E, Kennis JTM, van Stokkum IHM, Cogdell RJ, van Grondelle R (2002) An alternative carotenoid-to-bacteriochlorophyll energy transfer pathway in photosynthetic light harvesting. *Proc Natl Acad Sci USA* 99:6017–6022.
32. Frank HA, et al. (2000) Effect of the solvent environment on the spectroscopic properties and dynamics of the lowest excited states of carotenoids. *J Phys Chem B* 104:4569–4577.
33. Zigmantas D, et al. (2004) Effect of a conjugated carbonyl group on the photophysical properties of carotenoids. *Phys Chem Chem Phys* 6:3009–3016.
34. Niedzwiedzki DM, Fuciman M, Frank HA, Blankenship RE (2011) Energy transfer in an LH4-like light harvesting complex from the aerobic purple photosynthetic bacterium *Roseobacter denitrificans*. *Biochim Biophys Acta* 1807:518–528.
35. Zigmantas D, Hiller RG, Yartsev A, Sundström V, Polívka T (2003) Dynamics of excited states of the carotenoid peridinin in polar solvents: Dependence on excitation wavelength, viscosity, and temperature. *J Phys Chem B* 107:5339–5348.
36. Enriquez MM, et al. (2010) The intramolecular charge transfer state in carbonyl-containing polyenes and carotenoids. *J Phys Chem B* 114:12416–12426.
37. Polívka T, Kerfeld CA, Pascher T, Sundström V (2005) Spectroscopic properties of the carotenoid 3′-hydroxyechinenone in the orange carotenoid protein from the cyanobacterium *Arthrospira maxima*. *Biochemistry* 44:3994–4003.
38. Wilson A, et al. (2010) Structural determinants underlying photoprotection in the photoactive orange carotenoid protein of cyanobacteria. *J Biol Chem* 285:18364–18375.
39. Chábera P, Durchan M, Shih PM, Kerfeld CA, Polívka T (2011) Excited-state properties of the 16 kDa red carotenoid protein from *Arthrospira maxima*. *Biochim Biophys Acta* 1807:30–35.
40. de Weerd FL, Dekker JP, van Grondelle R (2003) Dynamics of beta-carotene-to-chlorophyll singlet energy transfer in the core of photosystem II. *J Phys Chem B* 107:6214–6220.
41. Walla PJ, Linden PA, Ohta K, Fleming GR (2002) Excited-state kinetics of the carotenoid S_1 state in LHC II and two-photon excitation spectra of lutein and beta-carotene in solution: Efficient car S_1-Chl electronic energy transfer via hot S_1 states? *J Phys Chem A* 106:1909–1916.
42. Durchan M, et al. (2010) Carotenoids in energy transfer and quenching processes in Pcb and Pcb-PS I complexes from *Prochlorothrix hollandica*. *J Phys Chem B* 114:9275–9282.
43. Olsen JD, Sockalingum GD, Robert B, Hunter CN (1994) Modification of a hydrogen bond to a bacteriochlorophyll *a* molecule in the light-harvesting 1 antenna of *Rhodobacter sphaeroides*. *Proc Natl Acad Sci USA* 91:7124–7128.
44. Sturgis J, Olsen CN, Robert B, Hunter CN (1997) The functions of conserved tryptophan residues of the core light harvesting complex of *Rhodobacter sphaeroides*. *Biochemistry* 36:2772–2778.
45. Babst M, Albrecht H, Wegmann I, Brunisholz R, Zuber H (1991) Single amino acid substitutions in the B870 alpha and beta light- harvesting polypeptides of *Rhodobacter capsulatus*. Structural and spectral effects. *Eur J Biochem* 202:277–284.
46. Richter P, Brand M, Drews G (1992) Characterization of $LH1^-$ and $LH1^+$ *Rhodobacter capsulatus pufA* mutants. *J Bacteriol* 174:3030–3041.
47. Kleinschmidt M, Marian CM, Waletzke M, Grimme S (2009) Parallel multireference configuration interaction calculations on mini-beta-carotenes and beta-carotene. *J Chem Phys* 130:044708.
48. Koepke J, Hu XC, Muenke C, Schulten K, Michel H (1996) The crystal structure of the light-harvesting complex II (B800–850) from *Rhodospirillum molischianum*. *Structure* 4:581–597.
49. Di Mascio P, Kaiser S, Sies H (1989) Lycopene as the most efficient biological carotenoid singlet oxygen quencher. *Arch Biochem Biophys* 274:532–538.
50. Yurkov V, Csotonyi JT (2009) New light on aerobic anoxygenic phototrophs. *The Purple Phototrophic Bacteria*, eds CN Hunter, F Daldal, MC Thurnauer, and JT Beatty (Springer, Dordrecht), pp 31–55.
51. Jones MR, et al. (1992) Mutants of *Rhodobacter sphaeroides* lacking one or more pigment protein complexes and complementation with reaction centre, LH1, and LH2 genes. *Mol Microbiol* 6:1173–1184.
52. Ratcliffe EC, et al. (2011) Experimental evidence that the membrane-spanning helix of PufX adopts a bent conformation that facilitates dimerisation of the *Rhodobacter sphaeroides* RC-LH1 complex through N-terminal interactions. *Biochim Biophys Acta* 1807:95–107.
53. van Stokkum IHM, Larsen DS, van Grondelle R (2004) Global and target analysis of time-resolved spectra. *Biochim Biophys Acta Bioenerg* 1657:82–104.